Article

Molecular Cell

The F-box Protein KIB1 Mediates Brassinosteroid-Induced Inactivation and Degradation of GSK3-like Kinases in *Arabidopsis*

Graphical Abstract

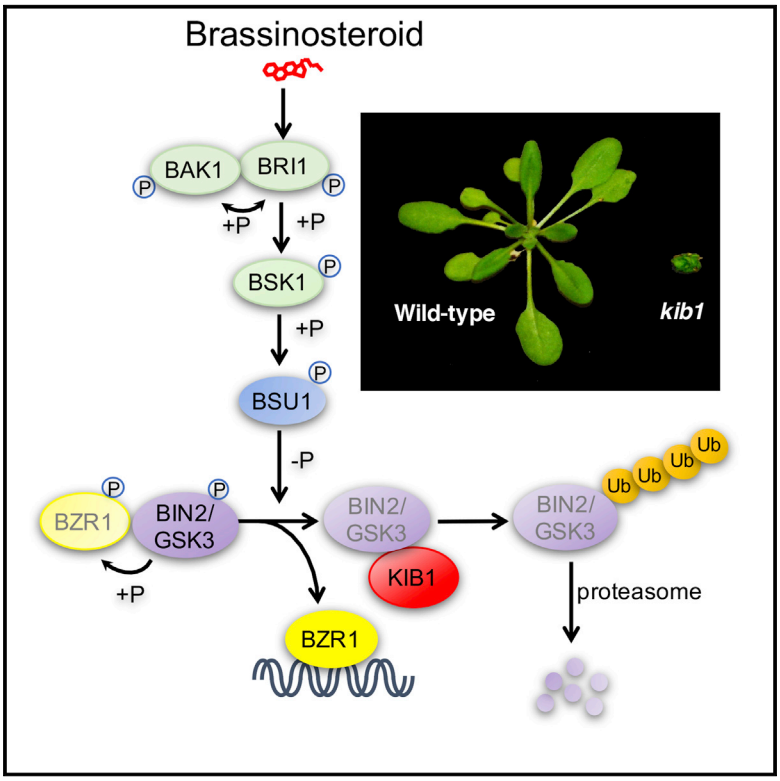

Highlights

- KIB1 is an essential positive regulator in brassinosteroid signaling
- KIB1 mediates BR-induced ubiquitination and degradation of GSK3 kinase BIN2
- KIB1 binding to BIN2 prevents BIN2-substrate interaction and promotes BIN2 degradation

Authors

Jia-Ying Zhu, Yuyao Li, Dong-Mei Cao, ..., Yang Bi, Shengwei Zhu, Zhi-Yong Wang

Correspondence

zywang24@stanford.edu

In Brief

Zhu et al. identify KIB1 as an F-box E3 ubiquitin ligase required for brassinosteroid signal transduction and further reveal a dual mechanism of KIB1-mediating GSK3 inactivation: blocking substrate access by the same binding event that leads subsequently to its ubiquitination and proteasomal degradation.

Zhu et al., 2017, Molecular Cell *66*, 648–657
June 1, 2017
http://dx.doi.org/10.1016/j.molcel.2017.05.012

CellPress

Molecular Cell
Article

The F-box Protein KIB1 Mediates Brassinosteroid-Induced Inactivation and Degradation of GSK3-like Kinases in *Arabidopsis*

Jia-Ying Zhu,[1] Yuyao Li,[1] Dong-Mei Cao,[2,3] Hongjuan Yang,[1,2] Eunkyoo Oh,[1,4] Yang Bi,[1,5] Shengwei Zhu,[1,2] and Zhi-Yong Wang[1,6,*]

[1]Department of Plant Biology, Carnegie Institution for Science, Stanford, CA 94305, USA
[2]Key Laboratory of Plant Molecular Physiology, Institute of Botany, Chinese Academy of Sciences, Beijing 100093, China
[3]Institute of Horticulture, Shanxi Academy of Agriculture Sciences, Taiyuan 030031, China
[4]Department of Bioenergy Science and Technology, Chonnam National University, Gwangju 61186, South Korea
[5]Department of Biology, Stanford University, Stanford, CA 94305, USA
[6]Lead Contact
*Correspondence: zywang24@stanford.edu
http://dx.doi.org/10.1016/j.molcel.2017.05.012

SUMMARY

The glycogen synthase kinase-3 (GSK3) family kinases are central cellular regulators highly conserved in all eukaryotes. In *Arabidopsis*, the GSK3-like kinase BIN2 phosphorylates a range of proteins to control broad developmental processes, and BIN2 is degraded through unknown mechanism upon receptor kinase-mediated brassinosteroid (BR) signaling. Here we identify KIB1 as an F-box E3 ubiquitin ligase that promotes the degradation of BIN2 while blocking its substrate access. Loss-of-function mutations of KIB1 and its homologs abolished BR-induced BIN2 degradation and caused severe BR-insensitive phenotypes. KIB1 directly interacted with BIN2 in a BR-dependent manner and promoted BIN2 ubiquitination in vitro. Expression of an F-box-truncated KIB1 caused BIN2 accumulation but dephosphorylation of its substrate BZR1 and activation of BR responses because KIB1 blocked BIN2 binding to BZR1. Our study demonstrates that KIB1 plays an essential role in BR signaling by inhibiting BIN2 through dual mechanisms of blocking substrate access and promoting degradation.

INTRODUCTION

As sessile organisms, plants need exceptionally high levels of developmental plasticity, which require sophisticated signaling mechanisms. Plant growth is controlled by integrating complex environmental signals with endogenous hormones (Chaiwanon et al., 2016). Among these, brassinosteroid (BR) is a major growth-promoting hormone that integrates information about internal nutrient/energy status with other hormonal and environmental signals (Chaiwanon et al., 2016; Zhang et al., 2016). BR activation of the BRI1 receptor kinase initiates a phosphorylation cascade that leads to inhibition of the glycogen synthase kinase-3 (GSK3)-like kinase BIN2 (Kim and Wang, 2010; Zhu et al., 2013). BIN2 phosphorylates and regulates other kinases and a number of key transcription factors, thereby playing a central role in BR regulation of gene expression and specific cellular and developmental processes (Li and Nam, 2002; Youn and Kim, 2015).

Among the BIN2 regulated transcription factors, the BRISSINOZOLE-RESISTANT 1 (BZR1) family of transcription factors plays a major role in BR promotion of plant growth, as dominant mutations that cause constitutive activation of BZR1 or its homolog BZR2 (also named BES1) suppress most of the growth defects of the BR-deficient and -insensitive mutants (Wang et al., 2002; Yin et al., 2002). BZR1 binds to thousands of BR-responsive promoters (Sun et al., 2010) and regulates their expression by interacting with other transcription regulators (Oh et al., 2014a, 2014b). BIN2 phosphorylation inhibits BZR1 nuclear localization and DNA-binding activity (Gampala et al., 2007; Vert and Chory, 2006), whereas upon BR inactivation of BIN2, protein phosphatase 2A (PP2A) dephosphorylates BZR1 to enable BR-responsive gene expression (Sun et al., 2010; Tang et al., 2011; Wang et al., 2012). The accumulation of BZR1 and activity of BIN2 are also regulated by sugar signaling mediated by the target of rapamycin (TOR) pathway, which allows nutrient/energy signaling to modulate steroid-dependent growth (Xiong et al., 2017; Zhang et al., 2016). In addition to BZR1, BIN2 also phosphorylates the PHYTOCHROME INTERACTING FACTOR 4 (PIF4), AUXIN RESPONSE FACTOR 2 (ARF2), and CESTA transcription factors to regulate cell elongation (Bernardo-García et al., 2014; Khan et al., 2014; Vert et al., 2008), the AUXIN RESPONSE FACTOR 7 (ARF7) to modulate lateral root development (Cho et al., 2014), and the ENHANCER OF GLABRA 3 (EGL3) and TRANSPARENT TESTA GLABRA1 (TTG1) factors to regulate root hair formation (Cheng et al., 2014). Further, BIN2 phosphorylates components of a mitogen-activated protein (MAP) kinase pathway to mediate BR regulation of stomata development (Gudesblat et al., 2012; Khan et al., 2013; Kim et al., 2012) and phosphorylates the SnRK2 kinases to modulate plant responses to the stress hormone abscisic

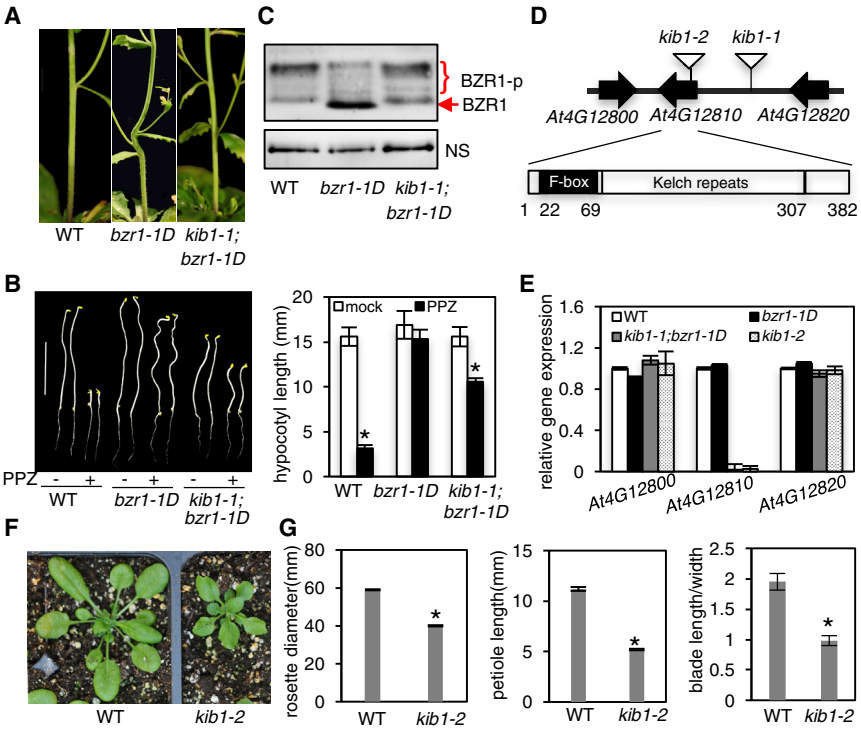

Figure 1. The *kib1* Mutation Suppresses *bzr1-D* Phenotype by Increasing the Phosphorylation of BZR1

(A) The *kib1* mutation suppresses the stem-bending phenotype of *bzr1-1D*. Stems of 8-week-old plants of wild-type (WT), *bzr1-1D*, and *kib1-1;bzr1-1D* are shown.

(B) *kib1-1;bzr1-1D* is less resistant to propiconazole (PPZ) than *bzr1-1D*. Left: seedlings of the indicated genotypes grown on the medium with or without 2 μM PPZ in the dark for 5 days. Scale bar, 10 mm. Right: the quantitation of hypocotyl lengths in the indicated genotypes.

(C) Immunoblot analysis of phosphorylated (BZR1-p) and de-phosphorylated BZR1 in 7-day-old light-grown seedlings of the indicated genotypes using an anti-BZR1 antibody. Nonspecific bands (NS) show protein loadings.

(D) Diagrams of the T-DNA insertion sites in *kib1-1*and *kib1-2* mutants (top) and a gene model of *KIB1* (bottom).

(E) qRT-PCR analysis of the expression levels of *KIB1* and its neighbor genes in the indicated genotypes. The data are shown as means of three biological repeats ± SD.

(F) Plant morphology of WT and *kib1-2* grown in the soil for 3 weeks.

(G) Quantification of the rosette diameters, petiole lengths, and ration between blade length and blade width of WT and *kib1-2* plants. The rosette diameters are measured from 3-week-old plants grown in a long-day condition. Petiole lengths, blade lengths, and blade widths were determined for the sixth leaves.

The data in (B) and (G) are shown as means ± SD, n = 15. The asterisks indicate significant differences by Student's t test (*$p < 0.05$) when compared to wild-type. Also see Figures S1–S3.

acid (Cai et al., 2014). These observations indicate that BIN2 plays a central role in cellular and developmental regulation, and therefore, regulation of BIN2 level is crucial for growth and stress adaptation in plants.

Despite BIN2's central function and extensive studies of the BR signaling pathway, the mechanisms by which BR restrains cellular BIN2 level are not fully understood. Upon BR binding and activation (Hothorn et al., 2011; She et al., 2011), BRI1 phosphorylates the BR-SIGNALING KINASE1 (BSK1) and the CONSTITUTIVE DIFFERENTIAL GROWTH 1 (CDG1) kinase (Kim et al., 2011; Tang et al., 2008), which in turn phosphorylate and activate the BRI1 SUPPRESSOR 1 (BSU1) phosphatase (Kim et al., 2009, 2011). BSU1 dephosphorylates BIN2 at Tyr200 to reduce its kinase activity (Kim et al., 2009). There is evidence that BR signaling involves proteasome-mediated BIN2 degradation (Peng et al., 2008), and interestingly, glucocorticoid also promotes GSK3 degradation in mammalian cells (Dominguez and Green, 2000; Failor et al., 2007). However, the protein factors and molecular mechanisms for regulating GSK3 degradation have remained unknown.

In this study, we report the identification of an E3 ubiquitin ligase for GSK3s as an essential component of the BR signaling pathway in *Arabidopsis*. Genetic analysis demonstrates that KIB1 is essential for BR signaling and specifically for BR-induced BIN2 degradation. Biochemical analyses revealed that KIB1 not only mediates BIN2 ubiquitination, but also blocks its substrate access. Our study demonstrates that BR signaling induces KIB1-BIN2 interaction, which directly prevents BIN2 interacting with its substrate and subsequently causes BIN2 ubiquitination and degradation.

RESULTS

Loss-of-Function *kib1* Mutation Suppresses *bzr1-1D* and Increases BZR1 Phosphorylation

The dominant gain-of-function *bzr1-1D* mutation (containing P234L substitution) enhances BZR1's interaction with PP2A and hence its dephosphorylation (Tang et al., 2011), causing constitutive BR-response phenotypes, including BR-independent hypocotyl elongation and stem kink due to organ fusion (Gendron et al., 2012; Wang et al., 2002) (Figure 1A). Genetic mutations that enhance BIN2 kinase activity or increase BIN2 protein level are expected to increase phosphorylation of bzr1-1D and suppress the *bzr1-1D* phenotypes. We thus screened for transfer DNA (T-DNA)-mutagenized suppressors of *bzr1-1D* (Fan et al., 2012) and identified a mutant that showed no kink at the stem-branch junctions (Figure 1A). We named the mutation *kink suppressed in bzr1-1D* (*kib1-1*). The *kib1-1* mutation also suppressed the other phenotypes of *bzr1-1D*, including the resistance to BR biosynthesis inhibitor propiconazole (PPZ) (Figure 1B) and late-flowering phenotypes (Figures S1A and S1B). The suppression of multiple phenotypes of *bzr1-1D* suggests that *kib1-1* mutation affects the protein level or activity of bzr1-1D. Indeed, immunoblot analysis showed that the

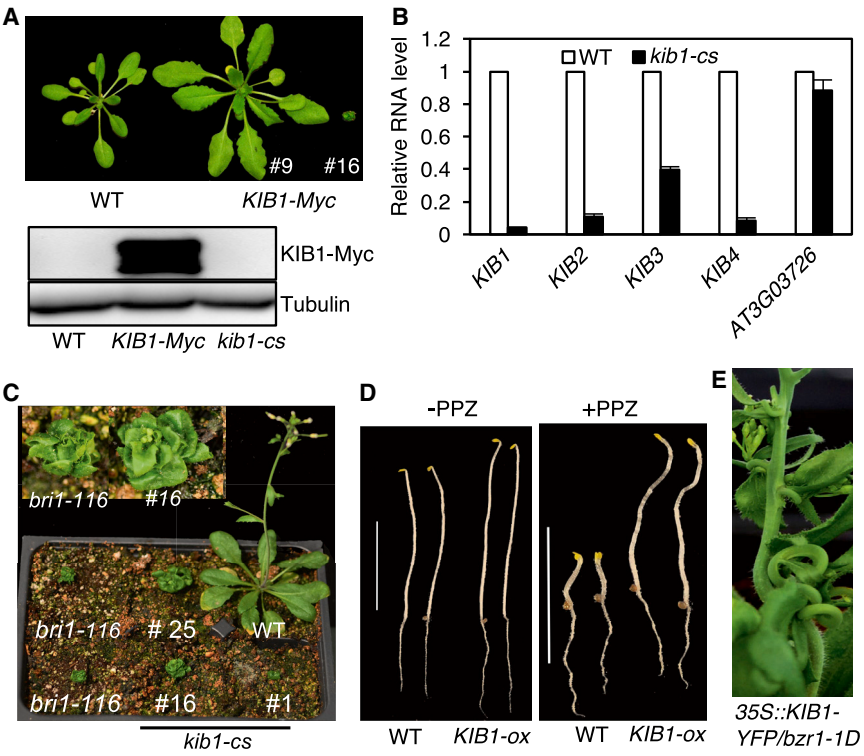

Figure 2. KIB1 Plays a Positive Role in the BR Signal Transduction Pathway

(A) Plant morphology and KIB1-Myc protein levels of 3-week-old WT and two independent *KIB1-Myc* transgenic *Arabidopsis* (#9 and #16). Tubulin protein levels show the protein loadings.

(B) qRT-PCR analysis of the expression level of *KIB1* and its homologs in WT and *KIB1-Myc* (#16) co-suppression line (*kib1-cs*). The data are shown as means of three biological repeats ± SD.

(C) 4-week-old plants of *KIB1-Myc* co-suppression lines (#1, #16, and #25), WT, and *bri1-116* mutant. Inset shows close-up view.

(D) *KIB1* overexpression line is insensitive to PPZ. WT and *KIB1-ox* transgenic plants were grown on the medium with (+) or without (–) 2 μM PPZ in the dark for 7 days. Scale bar, 10 mm.

(E) A transgenic plant overexpressing *KIB1* in the *bzr1-1D* mutant shows severe stem-bending phenotype.

Also see Figure S4.

kib1-1;bzr1-1D double mutant accumulated more phosphorylated BZR1 and less unphosphorylated BZR1 protein than the *bzr1-1D* single mutant (Figure 1C). The results suggest that the *kib1-1* mutation increased BZR1 phosphorylation.

We next investigated the nature of the *kib1-1* mutation. Using thermal asymmetric interlaced PCR (Liu et al., 1995), we identified a T-DNA flanking sequence in the promoter of *AT4G12810* in the *kib1-1;bzr1-1D* mutant (Figure 1D). Quantitative RT-PCR analysis showed that the expression level of *AT4G12810* was greatly reduced in *kib1-1;bzr1-1D*, whereas the expression levels of its neighboring genes *AT4G12800* and *AT4G12820* were not affected (Figure 1E). To confirm that loss of *AT4G12810* expression is responsible for the *kib1-1* phenotype, we obtained another T-DNA insertion mutant *kib1-2* (SAIL_1230_F06), in which a T-DNA was inserted in an exon of *AT4G12810* (Figure 1D). Quantitative RT-PCR analysis detected no expression of *AT4G12810* in *kib1-2* (Figure 1E). We crossed *kib1-2* to the *bzr1-1D* mutant, and *kib1-2;bzr1-1D* double mutant had straight stems (Figure S1C), indicating that, similar to *kib1-1*, *kib1-2* suppresses the stem kink phenotype of *bzr1-1D*. Homozygous *kib1-2* mutants showed shorter hypocotyls compared to wild-type seedlings grown on the medium (Figures S1D and S1E). Expressing *KIB1-YFP* under the *KIB1* native promoter in *kib1-2* mutant restored the mutant hypocotyl phenotype (Figures S1D and S1E). *kib1-2* displayed rosette leaves with shorter petioles and wider, but shorter, leaf blades when grown in the soil (Figures 1F and 1G), thus resembling weak BR-deficient mutants. These results confirm that loss of *AT4G12810* function is responsible for the *bzr1-1D*-suppression phenotypes of *kib1-1* and *kib1-2*, and thus we named *AT4G12810* gene *KIB1*.

KIB1 encodes a 382 aa protein that is a member of the F-box family protein, and *KIB1* has three closest homologous genes that we named *KIB2*, *KIB3*, and *KIB4* (Figure S2A). KIB1 and its homologs contain a putative F-box domain at the N-terminal region and three kelch repeats at the C-terminal region (Figure 1D; Figure S2B). The expression pattern of *KIB1* was examined using KIB1 promoter fused with GUS reporter gene. GUS stain results showed *KIB1* expression broadly in various tissues, including young seedlings, leaves, stems, flower buds, and flowers (Figure S3A). A KIB1-YFP (yellow fluorescent protein) fusion protein expressed from *KIB1 promoter* (*KIB1::KIB1-YFP*) in transgenic plants showed a strong signal in the nucleolus and weaker signal in the cytoplasm (Figure S3B).

KIB1 Is an Essential Component for BR Signaling

To further analyze the function of KIB1, we transformed wild-type *Arabidopsis* with T-DNA constructs that overexpressed KIB1 fused to the Myc tag (*KIB1-Myc*) or the yellow fluorescence protein (*KIB1-YFP*) from the constitutive 35S promoter. With both constructs, we obtained more than 30 transgenic plants that had larger rosette leaves with longer petioles compared to wild-type (Figure 2A; Figures S4A and S4B) and three transgenic plants that were extreme dwarfs resembling the BR receptor mutant *bri1* (Figures 2A–2C; Figure S4C). Immunoblotting analysis detected KIB1-Myc overexpression in the larger plants, but not in the dwarf plants (Figure 2A). Quantitative RT-PCR analysis showed that the dwarf plants had greatly reduced expression of *KIB1* and its three closest homologous genes *KIB2*, *KIB3*, and *KIB4* (Figure 2B). These results show that the larger plants were KIB1 overexpression (*KIB1-ox*) lines and the dwarf plants were KIB1 cosuppression (*kib1-cs*) lines. The *KIB1-ox* seedlings displayed longer hypocotyls compared to wild-type (Figures S4D and S4E), while the hypocotyl lengths of *kib1-cs* seedlings were severely short (Figures S4D and S4E). The *KIB1-ox* lines were insensitive to the BR biosynthesis inhibitor PPZ, similar to *bzr1-1D* and BIN2 loss-of-function triple

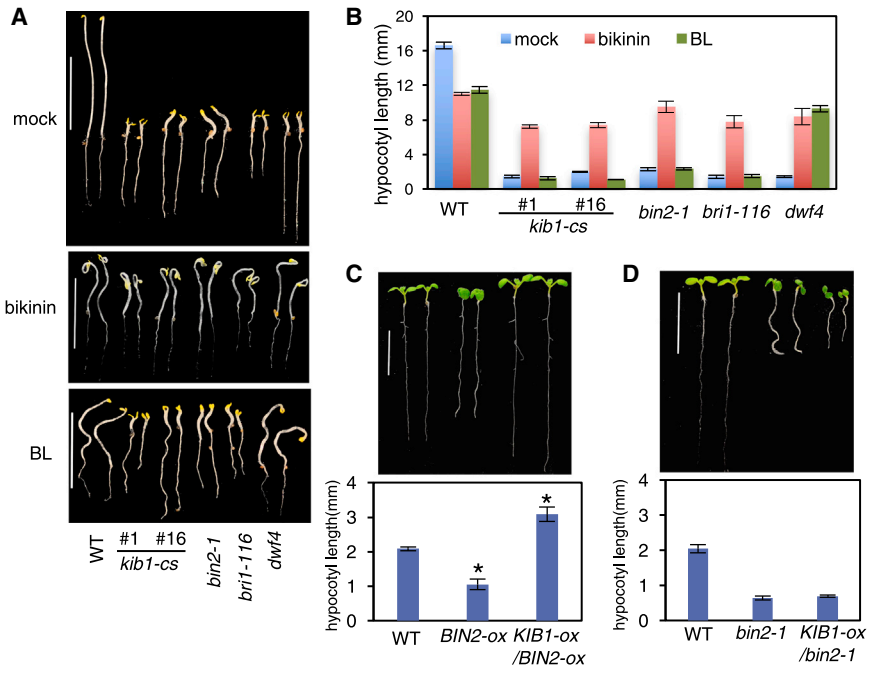

Figure 3. KIB1 Acts Upstream of BIN2 in the BR Signaling Pathway

(A and B) The *kib1-cs* mutant is rescued by bikinin treatment, but not BL treatment. Morphology (A) and hypocotyl length measurement (B) of the indicated genotype seedlings grown on the medium containing bikinin (30 μM), BL (1 μM), or mock solution in the dark for 5 days.

(C and D) Overexpression of *KIB1* partially rescues the *BIN2-ox* transgenic *Arabidopsis*, but not the *bin2-1* mutant. Morphology (top) and hypocotyl length measurement (bottom) of 7-day-old light-grown seedlings of the indicated genotypes.

The data in (B), (C), and (D) are shown as means ± SD, n = 15. The asterisks indicate significant differences by Student's t test (*$p < 0.05$) when compared to wild-type.

Also see Figure S5.

mutant *bin2-3bil1bil3* (Figure 2D; Figures S4F and S4G). Overexpression of *KIB1-YFP* in the *bzr1-1D* mutant background severely enhanced the stem-bending phenotype of *bzr1-1D* (Figure 2E). These results demonstrate that overexpression of *KIB1* activates the BR signal transduction pathway.

To determine the step of BR signal transduction that KIB1 acts on, we compared the *kib1-cs* plants with BR biosynthetic and signaling mutants for their morphology and responses to BR and bikinin, a chemical inhibitor of GSK3 kinases (De Rybel et al., 2009). The *kib1-cs* plants, grown under the light or in the dark, had phenotypes nearly identical to the BR insensitive mutants *bri1-116* and *bin2-1* or the BR-deficient mutant *dwf4* (Figures 2C and 3A; Figures S4C–S4G). The *dwf4* mutant, which is deficient in BR synthesize, was rescued by brassinolide (BL, the most active form of BR), whereas *bri1-116* and *bin2-1*, in which BIN2 is not inactivated by BL (Kim et al., 2009), were only rescued by bikini, but not by BL (Figures 3A and 3B). Similar to *bri1-116* and *bin2-1*, the *kib1-cs* seedlings were insensitive to BL but were rescued by bikinin (Figures 3A and 3B), suggesting that *kib1-cs* is defective in BR inactivation of BIN2. The results demonstrate that KIB1, together with its close homologs, is required for BR signal transduction upstream of BIN2. Consistent with this notion, *KIB1* overexpression suppressed the dwarf phenotypes of transgenic plants overexpressing wild-type *BIN2* (Kim et al., 2009) (Figure 3C) but did not suppress the strong dwarf phenotypes of the homozygous dominant *bin2-1* mutant (Figure 3D; Figure S5), possibly because KIB1 inhibits wild-type BIN2, but not the mutant bin2-1, which contains E263K substitution (Peng et al., 2008).

KIB1 Promotes BR-Induced BIN2 Degradation

KIB1 contains a putative F-box motif (Figure 1D; Figure S2B), a structure found in many E3 ubiquitin ligases (Cardozo and Pagano, 2004; Gagne et al., 2002). To test whether KIB1 functions as an E3 ubiquitin ligase that promotes BIN2 degradation, we analyzed the effects of overexpression and loss of function of *KIB1* on the level of BIN2 protein. Immunoblot analysis showed that overexpression of *KIB1-Myc* decreased the BIN2-YFP protein level dramatically in transgenic *Arabidopsis* (Figure 4A), whereas quantitative RT-PCR analysis showed no obvious effect on *BIN2-YFP* RNA level (Figure 4B). Furthermore, we found that the endogenous BIN2 protein level was decreased in the *KIB1-ox* line (Figure 4C), which correlated with increased levels of the unphosphorylated form of BZR1 (Figure 4C), similar to that observed in the *bin2-3bil1bil2* triple mutant (Figure 4C). In contrast, the *kib1-cs* plants showed an increased level of BIN2 and enhanced BZR1 phosphorylation, similar to the gain-of-function mutant *bin2-1* (Figure 4C). These results demonstrate that KIB1 promotes BIN2 degradation, leading to subsequent accumulation of unphosphorylated BZR1.

Previous studies showed that BR induces BIN2 degradation by the proteasome (Peng et al., 2008). We therefore further tested whether KIB1 is required for BR-induced BIN2 degradation. Consistent with the previous reports (Peng et al., 2008), we observed BR-induced degradation of BIN2 in wild-type plants (Figure 4D). However, BR had very little effect on BIN2 level in the *kib1-cs* plants, similar to the *bin2-1* dominant mutant (Figure 4D). By contrast, the *KIB1-ox* plants had a lower level of BIN2 than wild-type plants (Figure 4E). Treatment with the proteasome inhibitor MG132 increased BIN2 levels in the wild-type and *KIB1-ox* plants, but not in *kib1-cs* (Figure 4E). These results indicate that KIB1 is required for BR-induced BIN2 degradation by the proteasome.

KIB1 Is an E3 Ubiquitin Ligase for GSK3s

We next tested whether KIB1 interacts with BIN2. Yeast two-hybrid assays showed that BIN2 interacted with both the full-length KIB1 (KIB1F) and its C-terminal region containing three kelch repeats (amino acid 71–382, KIB1C), but not the N-terminal F-box domain (amino acid 1–70, KIB1N) (Figure 5A; Figures S6A and S6B). In contrast, the N-terminal F-box domain of KIB1

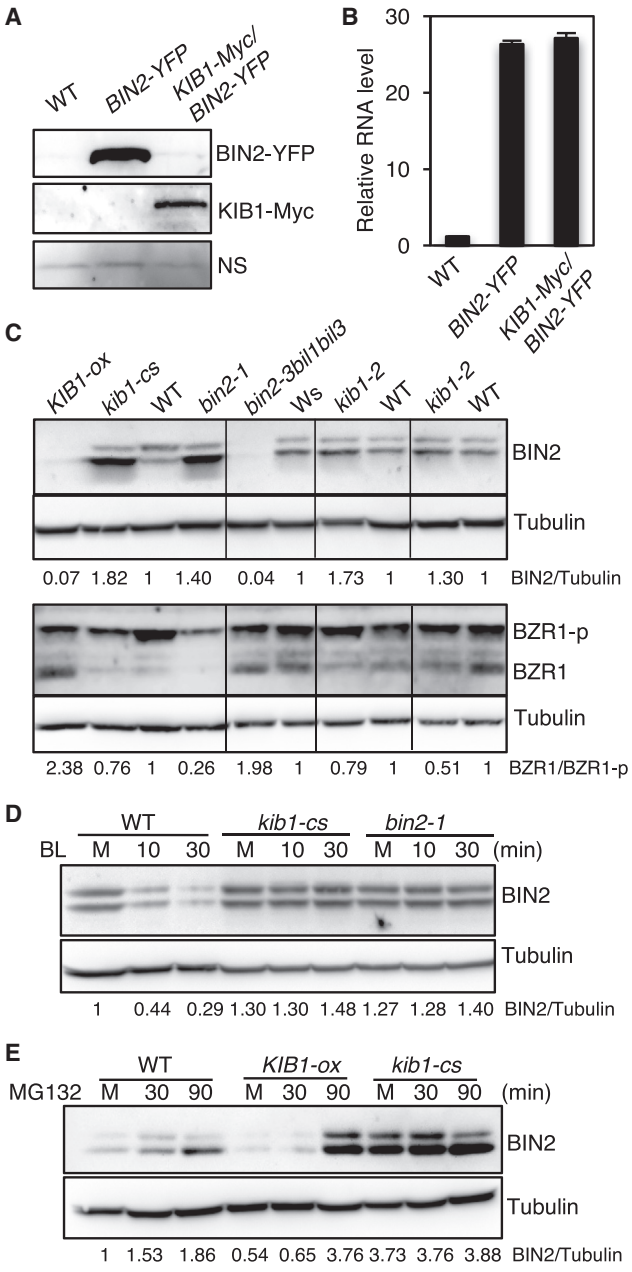

Figure 4. KIB1 Is Required for BR-Induced BIN2 Degradation

(A) Overexpression of *KIB1* decreased BIN2 protein level. Immunoblot shows BIN2-YPF and KIB1-Myc protein levels in the 7-day-old *BIN2-YFP* and *KIB1-Myc*/*BIN2-YFP* transgenic *Arabidopsis* using the anti-GFP or anti-Myc antibody. Nonspecific bands (NS) show the protein loadings.

(B) Quantitative RT-PCR analysis of the expression level of *BIN2* in the plants from (A). The gene expression levels were normalized to *PP2A* and presented as values relative to that of WT. The data are shown as means of three biological repeats ± SD.

(C) Immunoblot analyses of BIN2, phosphorylated (BZR1-p), and de-phosphorylated BZR1 (BZR1) levels of 10-day-old seedlings of the indicated genetic backgrounds using the anti-BIN2, anti-BZR1, or anti-tubulin antibody. The numbers below the blots indicate the relative ratios of the signal intensity between BIN2 and tubulin bands (BIN2/Tubulin) or the ratios of the signal intensity between de-phosphorylated BZR1 and phosphorylated BZR1 (BZR1/BZR1-p) bands. The ratios were normalized to WT control for each set of experiments.

(D and E) KIB1 is required for BR-induced BIN2 degradation by the proteasome. 10-day-old seedlings of WT, *kib1-cs*, and *bin2-1* grown on the medium with 2 μM PPZ under the light were treated with mock solution for 30 min (M) or with BL (100 nM) for 10 and 30 min (D). 7-day-old seedlings of WT, *KIB1-ox*, and *kib1-cs* grown under the light were treated with mock solution (M, 30 min) or with 10 μM MG132 (30 or 90 min) (E). The immunoblots were probed with the anti-BIN2 antibody or anti-tubulin antibody. The numbers below the blots indicate the relative ratios of the signal intensity between BIN2 and tubulin bands (BIN2/Tubulin).

interacted with the *Arabidopsis* SKP1-like1 (ASK1) (Gagne et al., 2002) (Figure 5A), which is consistent with the F-box motif being known to interact with the SKP1 core component to form the SKP1-Cullin-F-box (SCF) E3 ubiquitin ligase complex (Cardozo and Pagano, 2004). In addition, KIB1C interacted with several other *Arabidopsis* GSK3 family members (AtASK11, 12, 13, 22, and 23) (Figure S6A), and these *Arabidopsis* GSK3s have been shown to interact with BZR1 in yeast two-hybrid assays and to play redundant roles with BIN2 in BR signaling (Kim et al., 2009). Similarly, KIB2 also interacted with BIN2 in yeast (Figure S6C). In co-immunoprecipitation assays, BIN2 was detected after GFP-nAb immunoprecipitation using extracts from *KIB1::KIB1-YFP* transgenic plants, but not from wild-type plants (Figure 5B), indicating that KIB1 associates with BIN2 in vivo. To determine whether KIB1 is an E3 ligase for BIN2, we performed in vitro ubiquitination assays, and the results showed that KIB1 indeed can mediate BIN2 ubiquitination (Figure 5C).

Previous studies showed that phosphorylation of Tyr200 is required for full BIN2 kinase activity (Kim et al., 2009) and that the *bin2-1* mutation (E263K) blocks BR-induced BIN2 degradation (Peng et al., 2008). We thus tested whether Y200F and E263K substitutions affect BIN2 interaction with KIB1. KIB1-Myc pulled down BIN2 in vitro (Figure 5D). While the Y200F mutation showed no obvious effect on KIB1-BIN2 interaction, the *bin2-1* mutation reduced the KIB1-BIN2 interaction (Figure 5D). Similarly, in yeast, KIB1 and its homolog KIB2 interacted strongly with the wild-type BIN2, but only weakly with bin2-1 (Figures S6B and S6C). The reduced KIB1 interaction with bin2-1 is consistent with the dwarf phenotype of *KIB1-ox/bin2-1* (Figure 3D; Figure S5), which suggests that KIB1 is unable to inactivate bin2-1. Together, the results provide genetic evidence supporting the requirement of interaction with KIB1 for BR-induced BIN2 degradation.

KIB1 Binding Blocks BIN2 Access to Its Substrate BZR1

Deletion of F-box sequences has been shown to create a dominant-negative form of E3 ligase that interacts with substrate but is unable to mediate its ubiquitination, thus causing substrate accumulation (Yaron et al., 1998). We overexpressed an F-box-truncated KIB1 (KIB1C) fused with YFP in *Arabidopsis* (*KIB1C-YFP*). Surprisingly, the transgenic seedlings showed constitutive BR-response phenotypes, such as stem kinks (Figure 6A), insensitivity to BR biosynthesis inhibitor PPZ (Figure 6B), and large and curly leaves (Figure S7A), similar to *bzr1-1D* and plants overexpressing full-length *KIB1* (Figures 1 and 2). The *KIB1C-YFP* plants also displayed reduced lateral root development (Figures S7B and S7C), similar to the phenotypes observed in the

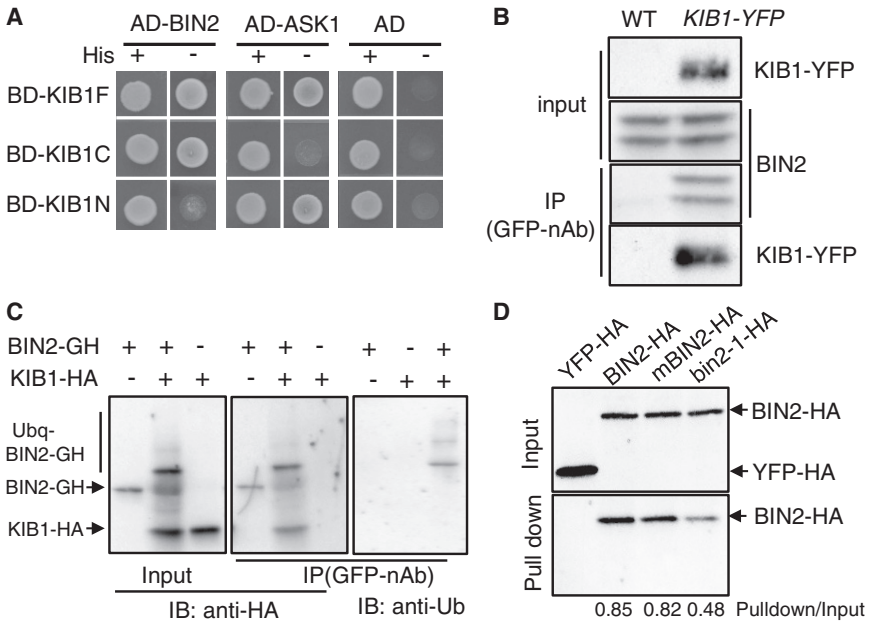

Figure 5. KIB1 Interacts with BIN2 and Promotes BIN2 Ubiquitination

(A) Yeast two-hybrid assay shows the interaction between the fragments of KIB1 and BIN2 or ASK1. KIB1F, full-length KIB1; KIB1N, amino acid 1–70; KIBC, amino acid 71–382.

(B) Co-immunoprecipitation assay shows that KIB1 is associated with BIN2 in vivo. Total proteins extracted from WT or *KIB1::KIB1-YFP* transgenic plants were immunoprecipitated with the GFP-nAb and then probed with the anti-GFP or anti-BIN2 antibody.

(C) In vitro ubiquitination assays show that KIB1 promotes BIN2 ubiquitination. BIN2-GFP-HA (BIN2-GH) was incubated with or without KIB1-HA for the ubiquitination assay reactions. The BIN2-GFP-HA protein was immunoprecipitated using the GFP-nAb and then analyzed by immunoblots using the anti-HA and anti-Ub antibody separately.

(D) In vitro pull-down assays show that KIB1 binds to BIN2. BIN2, BIN2Y200F (mBIN2), and bin2-1 fused with HA tags were pulled down by KIB1-YFP-HA immobilized on the GFP-nAb magnetic agarose beads and immunoblotted using an anti-HA antibody. YFP-HA was used as a negative control. The numbers below the blots indicate the ratio of the relative density between pull-down and input signals (Pulldown/Input).

Also see Figure S6.

bin2/gsk3 loss-of-function mutants (Cho et al., 2014). Consistent with the growth phenotype, the *KIB1C-YFP* plants accumulated increased levels of dephosphorylated BZR1 compared to wild-type both before and after BR treatment (Figure 6C). However, in contrast to the *KIB1-ox* plants in which BIN2 is degraded, these *KIB1C-YFP* plants accumulated a slightly increased level of BIN2 without BL treatment and did not show obvious BIN2 degradation upon BL treatment in contrast to the wild-type plants (Figure 6C). Thus, it appears that the F-box-truncated KIB1 caused BIN2 accumulation through a dominant negative effect but somehow decreased the phosphorylation of its substrate BZR1 (Figure 6C). One possibility is that KIB1 binding blocks BIN2 access to its substrate BZR1. Indeed, in vitro pull-down assays showed that BIN2 bound to BZR1 in the absence of KIB1 but bound to only KIB1, not BZR1, when both KIB1 and BZR1 were present (Figure 6D), indicating that KIB1 prevents BIN2 interaction with BZR1.

Consistent with the previous reports that BR signaling causes BIN2 degradation and BSU1-mediated dephosphorylation of BIN2 at pTyr200 (Kim et al., 2009; Peng et al., 2008), BL treatment of wild-type plants decreased the levels of BIN2 detected by both anti-BIN2 and anti-pTyr200-GSK3 antibodies (anti-pTyr, corresponding to Tyr279 and Tyr216 of human GSK3α/β) (Figure 6C). In contrast, BL treatment of the *KIB1C-YFP* plants had no obvious effect on BIN2 protein level but caused obvious dephosphorylation of BIN2 at pTyr200 (Figure 6C), suggesting that KIB1C-YFP abolished BIN2 degradation but did not interfere with BR-induced dephosphorylation of BIN2 at pTyr200. BL treatment also caused a mobility shift of KIB1C-YFP in immunoblot that can be mimicked by in vitro phosphatase treatment (Figure 6E; Figures S7D and S7E), indicating that BR induces KIB1 dephosphorylation. Further, co-immunoprecipitation assays showed that BR enhanced BIN2-KIB1C interaction (Figure 6E). These results suggest that the BR-induced dephosphorylation of pTyr200 is likely an upstream event that leads to BIN2 inactivation, KIB1 dephosphorylation, and BIN2-KIB1 interaction. Indeed, similar to BR, bikinin also caused BIN2 degradation (Figure 6F), suggesting that inhibiting BIN2 kinase activity is sufficient for triggering its degradation. Together, our results support a model that, upon BR signaling BSU1-mediated dephosphorylation and partial inactivation of BIN2, leads to recruitment of KIB1, which blocks BIN2 interaction with its substrates and further promotes BIN2 ubiquitination and degradation, ensuring robust signaling outputs (Figure 7).

DISCUSSION

Our study demonstrates that the KIB1 family F-box proteins are essential components of the BR signaling pathway, and they positively regulate BR signaling by both promoting ubiquitination/degradation and blocking substrate phosphorylation of GSK3 kinases. Previous studies demonstrated that GSK3 inactivation by BR signaling involves both BSU1-mediated dephosphorylation and proteasome-mediated BIN2 degradation (Kim et al., 2009; Peng et al., 2008). However, the functional importance and underlying mechanism of BIN2 degradation have remained unclear. Here our genetic evidence indicates that BR promotion of plant growth requires BIN2 degradation and inactivation mediated by KIB1. Further, we find that KIB1 binding with BIN2 not only mediates BR-induced ubiquitination and degradation of BIN2, but also directly blocks BIN2 access to its substrate BZR1. As such, our study reveals an essential step of BR signal transduction and uncovers dual mechanisms of GSK3 inhibition by its E3 ligase KIB1 through blocking substrate docking while

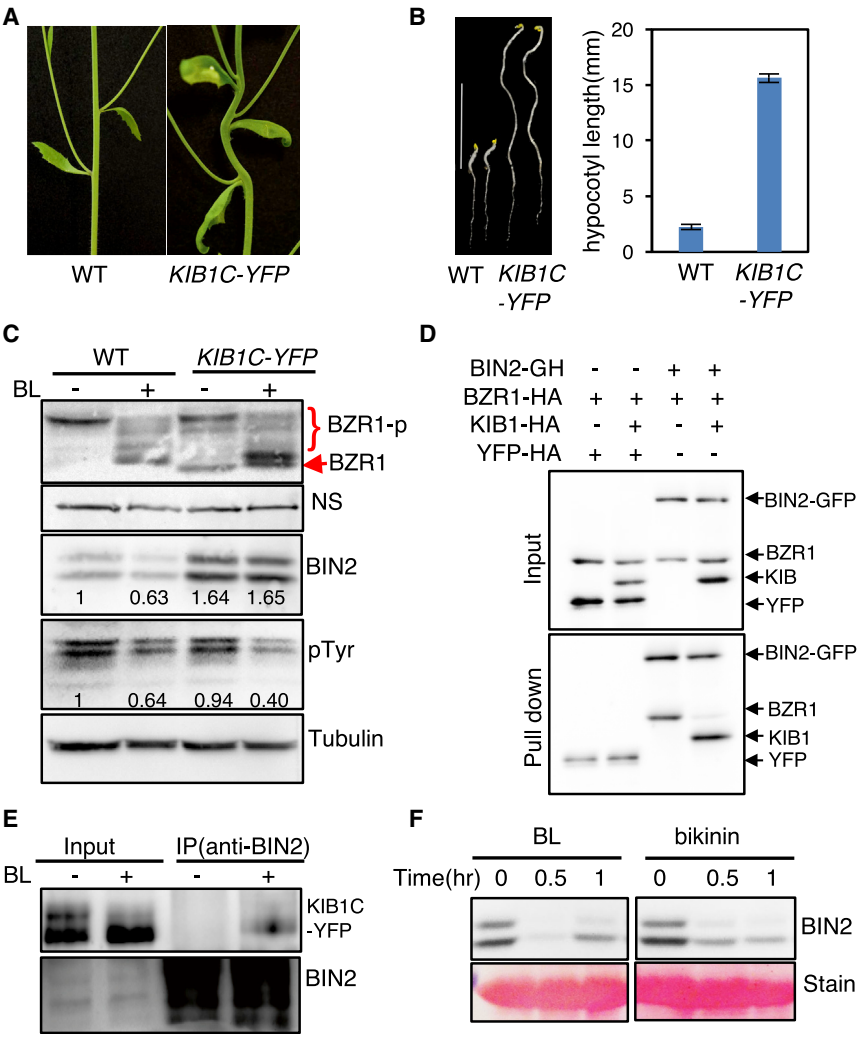

Figure 6. KIB1-BIN2 Interaction Blocks BIN2 Accessing Its Substrate BZR1

(A) *KIB1C-YFP* transgenic *Arabidopsis* grown under the light for 5 weeks shows stem bending.

(B) *KIB1C-YFP* transgenic *Arabidopsis* shows constitutive BR-response phenotypes. Left: 7-day-old seedlings of WT and *KIB1C-YFP* grown in the dark on the medium with or without 2 μM PPZ. Scale bar, 10 mm. Right: the quantitation of hypocotyl lengths in the indicated genotypes. The data are shown as means ± SD, n = 15.

(C) Immunoblot analyses of BZR1, BIN2, and phospho-GSK3 using the anti-BZR1, anti-BIN2, anti-pTyr279/Tyr216 (pTyr), or anti-tubulin antibody from 10-day-old seedlings of WT and *KIB1C-YFP* grown on the medium containing 2 μM PPZ (–) or 100 nM BL (+). Nonspecific bands (NS) and tubulin protein level show the equal loadings. The numbers inside the images indicate the relative ratios of the signal intensity between BIN2 or pTyr and tubulin bands. The ratio of WT was set to 1.

(D) In vitro pull-down assay shows that KIB1 blocks BIN2 binding to BZR1. The mixtures of the indicated proteins BZR1-HA, KIB1-HA, or YFP-HA were pulled down by BIN2-GFP-HA immobilized on the GFP-nAb magnetic agarose beads and analyzed by immunoblots using an anti-HA antibody. YFP-HA was used as a negative control.

(E) Co-immunoprecipitation assay shows that BR enhances BIN2-KIB1C interaction. Protein extracts from 7-day-old light-grown *KIBC-YFP* seedlings grown on the medium containing 2 μM PPZ treated with 100 nM BL or mock solution for 10 min were immunoprecipitated using an anti-BIN2 antibody and analyzed by immunoblots using an anti-GFP antibody.

(F) Inhibiting kinase activity of BIN2 by bikinin causes BIN2 degradation. Wild-type seedlings were grown on the medium containing 2 μM PPZ under the light for 10 days and then treated with 100 nM BL or 30 μM bikinin for the indicated time. Proteins were immunoblotted using an anti-BIN2 antibody. Ponceau S staining bands show the protein loadings.

Also see Figure S7.

promoting degradation. Together, the studies illustrate a model for tight regulation of GSK3/BIN2 by BR signaling through a combination of BSU1-mediated dephosphorylation and KIB1-mediated inhibition and degradation (Figure 7).

The functions of KIB1 are supported by strong genetic and biochemical evidence. Both in vitro and in vivo assays demonstrate that KIB1 directly interacts with BIN2 to promote BIN2 ubiquitination and subsequent degradation by the proteasome. Further, the interaction is enhanced by BR treatment in vivo, consistent with the role of KIB1 in BR promoting BIN2 degradation. The severe BR-insensitive dwarf phenotypes, BR-insensitive accumulation of BIN2, and increased phosphorylation of BZR1 observed in the *kib1-cs* plants clearly demonstrate the essential role for the KIB1 family proteins in BIN2 inactivation/degradation and BR signaling. The stronger phenotypes of *kib1-cs*, in which four homologous genes are suppressed, than the *kib1* single mutants, indicate that KIB1 family members redundantly fulfill an essential role in mediating BR signaling. Consistent with this notion, yeast two-hybrid assays showed that both KIB1 and its homolog KIB2 interact with BIN2, while KIB1 interacts with all six GSK3s that interact with BZR1 (Kim et al., 2009) (Figure S6). These results indicate that KIB1 and its homologs play similar roles in regulating GSK3s. Analysis of additional single and higher-order knockout mutants will be required to determine the degree of overlap between roles played by different KIB family members.

Regulation of cellular GSK3 level is likely to influence broadly GSK3-regulated processes. Further, KIB1 binding may block BIN2 access to specific substrates or non-selectively block all its substrates. The *KIB1C-YFP* plants displayed reduced lateral root development (Figures S7B and S7C), which is regulated through BIN2 phosphorylation of the ARF7 (Cho et al., 2014), suggesting that KIB1 also blocks BIN2 phosphorylation of ARF7. Therefore, KIB1 and its homologs may redundantly function as master regulators of GSK3s, impacting broadly GSK3-regulated processes in plants. Whether different KIB1 family members play distinct roles in different signaling and developmental context requires further genetic and molecular dissection.

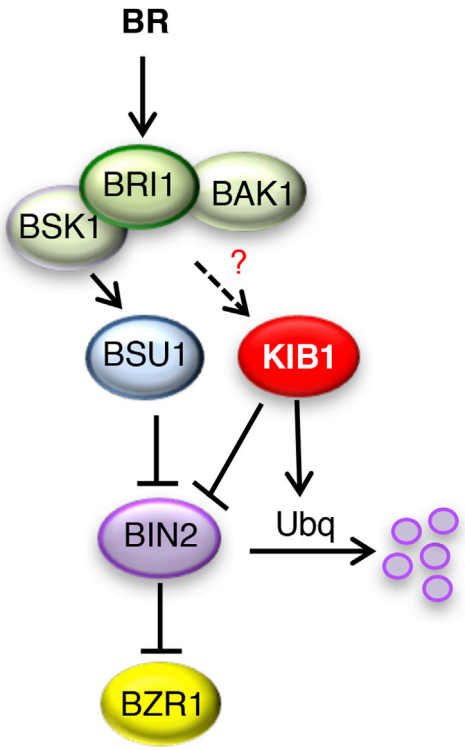

Figure 7. A Model for KIB1 Mediating BR-Induced BIN2 Inactivation and Degradation

BR activates the BRI1-BAK1 receptor kinase complex, triggering sequential phosphorylation of the BSK1 kinase and BSU1 phosphatase; BSU1 dephosphorylates BIN2 to reduce its kinase activity, which, through an unknown mechanism, leads to BIN2 binding by KIB1. KIB1 binding both excludes BIN2 association with its substrate BZR1 and facilitates the ubiquitination, leading to degradation, of BIN2. It remains unclear whether upstream BR signaling also modifies KIB1, such as by dephosphorylation, to enhance its interaction with BIN2.

Overexpression of an F-box-truncated KIB1, which binds BIN2 but lacks E3 ubiquitin ligase activity, caused BIN2 accumulation as expected but surprisingly resulted in phenotypes that are consistent with BIN2 inactivation, including decreased levels of BZR1 phosphorylation. A previous study has shown that BIN2 phosphorylation of its substrate BZR1 is mediated by a direct kinase-substrate docking mechanism (Peng et al., 2010). The in vitro binding competition assays showed that KIB1-BIN2 binding prevents BIN2-BZR1 interaction, revealing that KIB1 inhibits BIN2 by blocking substrate docking. Our study thus uncovers a mechanism of dual actions of E3 ubiquitin ligase: blocking substrate access while promoting ubiquitination/degradation. Such a dual mechanism of inactivation presumably provides rapid and efficient inhibition of BIN2, although the relative contributions of the "blocking" and "ubiquitination" activities in vivo remain unknown. Similar dual mechanisms may have been evolved broadly for other E3 ligase-substrate pairs but have been overlooked in research.

We have previously shown that BR-induced phospho-relay from BRI1, BSK1/CDG1, to BSU1 triggers BSU1 dephosphorylation of BIN2 at pTyr200 (Kim et al., 2009, 2011). However, mutating Tyr200 to Phe (Y200F) reduced, but did not fully abolish, BIN2 kinase activity based on in vitro kinase assays and the phenotypes of overexpression transgenic plants (Kim et al., 2009). This is consistent with additional mechanisms, such as KIB1-mediated inhibition and degradation, being required for effective BIN2 inactivation. The observations that BR induces pTyr200 dephosphorylation and BIN2-KIB1C interaction in the *KIB1C-YFP* plants suggest that BSU1-mediated dephosphorylation and inhibition of BIN2 kinase promotes its interaction with KIB1. Consistent with this notion is the observation that direct inactivation of BIN2 by its chemical inhibitor bikinin causes BIN2 degradation (Figure 6F). Since bikinin inhibits BIN2 as an ATP competitor (De Rybel et al., 2009), the results suggest that inhibiting BIN2 kinase activity is sufficient for triggering its degradation. While the Y200F mutation of BIN2 showed no obvious effect on KIB1 binding in vitro and in yeast (Figure 5D; Figures S6B and S6C), there is evidence that BIN2 is dephosphorylated at multiple residues upon BR treatment (Kim et al., 2009), and thus dephosphorylation at additional auto-phosphorylated residues other than Tyr200 may affect KIB1 binding. Alternatively, BIN2 phosphorylation of KIB1 might inhibit its E3 ubiquitin ligase function and thus stabilize BIN2. Our results support a model that, upon upstream BR signaling, an initial partial and/or reversible inactivation of BIN2 by BSU1-mediated dephosphorylation leads to further inhibition and eventual degradation mediated by KIB1, which are required for effective de-repression of BIN2 substrates such as BZR1.

It is interesting to note that glucocorticoid induces GSK3 ubiquitination/degradation in mammalian cells, and this involves phosphorylation of GSK3 by glucocorticoid-induced kinase (Sgk) and Akt kinases (Failor et al., 2007). In addition, a GSK3-binding protein (GBP) was shown to inhibit substrate phosphorylation and promote GSK3 depletion in *Xenopus* embryo patterning (Dominguez and Green, 2000; Farr et al., 2000). However, no E3 ubiquitin ligase that promotes GSK3 degradation in animals has been reported. While GSK3β has been shown to be ubiquitinated by the E3 ligase TNF receptor-associated factor 6 (TRAF6) in the Toll-like receptor 3 (TLR3)-mediated pro-inflammatory signaling pathway, such ubiquitination promotes assembly of functional signaling complex but has no effect on GSK3 degradation (Ko et al., 2015). In the Wnt signaling pathway, GSK3β is mono-ubiquitinated by ubiquitin E3 ligase β-TrCP, which suppresses recruitment of their substrate β-catenin without affecting GSK3β degradation (Gao et al., 2014). While the mechanisms for regulating GSK3 degradation remain obscure in animal systems, the KIB1-mediated regulation of BIN2 in the BR signaling pathway provides an example of how cell surface signaling regulates GSK3's stability as well as activity in plants.

STAR★METHODS

Detailed methods are provided in the online version of this paper and include the following:

- KEY RESOURCES TABLE
- CONTACT FOR REAGENT AND RESOURCE SHARING
- EXPERIMENTAL MODELS AND SUBJECT DETAILS

SUPPLEMENTAL INFORMATION

Supplemental Information includes seven figures and can be found with this article online at http://dx.doi.org/10.1016/j.molcel.2017.05.012.

AUTHOR CONTRIBUTIONS

J.-Y.Z., D.-M.C., and Z.-Y.W. conceived the projects. J.-Y.Z., Y.L., D.-M.C., H.Y., E.O., Y.B., and S.Z. performed the experiments. J.-Y.Z. and Z.-Y.W. wrote the manuscript.

ACKNOWLEDGMENTS

We thank Dr. Matthew Scott for helpful comments on the manuscript. This study was supported by a grant from NIH (R01GM066258) to Z.-Y.W.

Received: October 25, 2016
Revised: April 5, 2017
Accepted: May 10, 2017
Published: June 1, 2017

REFERENCES

Bernardo-García, S., de Lucas, M., Martínez, C., Espinosa-Ruiz, A., Davière, J.M., and Prat, S. (2014). BR-dependent phosphorylation modulates PIF4 transcriptional activity and shapes diurnal hypocotyl growth. Genes Dev. *28*, 1681–1694.

Cai, Z., Liu, J., Wang, H., Yang, C., Chen, Y., Li, Y., Pan, S., Dong, R., Tang, G., Barajas-Lopez, Jde.D., et al. (2014). GSK3-like kinases positively modulate abscisic acid signaling through phosphorylating subgroup III SnRK2s in Arabidopsis. Proc. Natl. Acad. Sci. USA *111*, 9651–9656.

Cardozo, T., and Pagano, M. (2004). The SCF ubiquitin ligase: insights into a molecular machine. Nat. Rev. Mol. Cell Biol. *5*, 739–751.

Chaiwanon, J., Wang, W., Zhu, J.Y., Oh, E., and Wang, Z.Y. (2016). Information integration and communication in plant growth regulation. Cell *164*, 1257–1268.

Cheng, Y., Zhu, W., Chen, Y., Ito, S., Asami, T., and Wang, X. (2014). Brassinosteroids control root epidermal cell fate via direct regulation of a MYB-bHLH-WD40 complex by GSK3-like kinases. eLife *3*, e02525.

Cho, H., Ryu, H., Rho, S., Hill, K., Smith, S., Audenaert, D., Park, J., Han, S., Beeckman, T., Bennett, M.J., et al. (2014). A secreted peptide acts on BIN2-mediated phosphorylation of ARFs to potentiate auxin response during lateral root development. Nat. Cell Biol. *16*, 66–76.

Choe, S., Dilkes, B.P., Fujioka, S., Takatsuto, S., Sakurai, A., and Feldmann, K.A. (1998). The DWF4 gene of Arabidopsis encodes a cytochrome P450 that mediates multiple 22α-hydroxylation steps in brassinosteroid biosynthesis. Plant Cell *10*, 231–243.

Clough, S.J., and Bent, A.F. (1998). Floral dip: a simplified method for Agrobacterium-mediated transformation of Arabidopsis thaliana. Plant J. *16*, 735–743.

Curtis, M., and Grossniklaus, U. (2003). A gateway cloning vector set for high-throughput functional analysis of genes in planta. Plant Physiol. *133*, 462–469.

De Rybel, B., Audenaert, D., Vert, G., Rozhon, W., Mayerhofer, J., Peelman, F., Coutuer, S., Denayer, T., Jansen, L., Nguyen, L., et al. (2009). Chemical inhibition of a subset of Arabidopsis thaliana GSK3-like kinases activates brassinosteroid signaling. Chem. Biol. *16*, 594–604.

Ding, X., Zhang, Y., and Song, W.Y. (2007). Use of rolling-circle amplification for large-scale yeast two-hybrid analyses. Methods Mol. Biol. *354*, 85–98.

Dominguez, I., and Green, J.B. (2000). Dorsal downregulation of GSK3beta by a non-Wnt-like mechanism is an early molecular consequence of cortical rotation in early Xenopus embryos. Development *127*, 861–868.

Failor, K.L., Desyatnikov, Y., Finger, L.A., and Firestone, G.L. (2007). Glucocorticoid-induced degradation of glycogen synthase kinase-3 protein is triggered by serum- and glucocorticoid-induced protein kinase and Akt signaling and controls beta-catenin dynamics and tight junction formation in mammary epithelial tumor cells. Mol. Endocrinol. *21*, 2403–2415.

Fan, X.Y., Sun, Y., Cao, D.M., Bai, M.Y., Luo, X.M., Yang, H.J., Wei, C.Q., Zhu, S.W., Sun, Y., Chong, K., and Wang, Z.Y. (2012). BZS1, a B-box protein, promotes photomorphogenesis downstream of both brassinosteroid and light signaling pathways. Mol. Plant *5*, 591–600.

Farr, G.H., 3rd, Ferkey, D.M., Yost, C., Pierce, S.B., Weaver, C., and Kimelman, D. (2000). Interaction among GSK-3, GBP, axin, and APC in Xenopus axis specification. J. Cell Biol. *148*, 691–702.

Felsenstein, J. (1989). PHYLIP - Phylogeny Inference Package (Version 3.2). Cladistics *5*, 164–166.

Gagne, J.M., Downes, B.P., Shiu, S.H., Durski, A.M., and Vierstra, R.D. (2002). The F-box subunit of the SCF E3 complex is encoded by a diverse superfamily of genes in Arabidopsis. Proc. Natl. Acad. Sci. USA *99*, 11519–11524.

Gampala, S.S., Kim, T.W., He, J.X., Tang, W., Deng, Z., Bai, M.Y., Guan, S., Lalonde, S., Sun, Y., Gendron, J.M., et al. (2007). An essential role for 14-3-3 proteins in brassinosteroid signal transduction in Arabidopsis. Dev. Cell *13*, 177–189.

Gao, C., Chen, G., Romero, G., Moschos, S., Xu, X., and Hu, J. (2014). Induction of Gsk3β-β-TrCP interaction is required for late phase stabilization of β-catenin in canonical Wnt signaling. J. Biol. Chem. *289*, 7099–7108.

Gendron, J.M., Liu, J.S., Fan, M., Bai, M.Y., Wenkel, S., Springer, P.S., Barton, M.K., and Wang, Z.Y. (2012). Brassinosteroids regulate organ boundary formation in the shoot apical meristem of Arabidopsis. Proc. Natl. Acad. Sci. USA *109*, 21152–21157.

Gudesblat, G.E., Schneider-Pizoń, J., Betti, C., Mayerhofer, J., Vanhoutte, I., van Dongen, W., Boeren, S., Zhiponova, M., de Vries, S., Jonak, C., and Russinova, E. (2012). SPEECHLESS integrates brassinosteroid and stomata signalling pathways. Nat. Cell Biol. *14*, 548–554.

Hothorn, M., Belkhadir, Y., Dreux, M., Dabi, T., Noel, J.P., Wilson, I.A., and Chory, J. (2011). Structural basis of steroid hormone perception by the receptor kinase BRI1. Nature *474*, 467–471.

Khan, M., Rozhon, W., Bigeard, J., Pflieger, D., Husar, S., Pitzschke, A., Teige, M., Jonak, C., Hirt, H., and Poppenberger, B. (2013). Brassinosteroid-regulated GSK3/Shaggy-like kinases phosphorylate mitogen-activated protein (MAP) kinase kinases, which control stomata development in Arabidopsis thaliana. J. Biol. Chem. *288*, 7519–7527.

Khan, M., Rozhon, W., Unterholzner, S.J., Chen, T., Eremina, M., Wurzinger, B., Bachmair, A., Teige, M., Sieberer, T., Isono, E., and Poppenberger, B. (2014). Interplay between phosphorylation and SUMOylation events determines CESTA protein fate in brassinosteroid signalling. Nat. Commun. *5*, 4687.

Kim, T.W., and Wang, Z.Y. (2010). Brassinosteroid signal transduction from receptor kinases to transcription factors. Annu. Rev. Plant Biol. *61*, 681–704.

Kim, T.-W., Guan, S., Sun, Y., Deng, Z., Tang, W., Shang, J.X., Sun, Y., Burlingame, A.L., and Wang, Z.-Y. (2009). Brassinosteroid signal transduction from cell-surface receptor kinases to nuclear transcription factors. Nat. Cell Biol. *11*, 1254–1260.

Kim, T.-W., Guan, S., Burlingame, A.L., and Wang, Z.-Y. (2011). The CDG1 kinase mediates brassinosteroid signal transduction from BRI1 receptor kinase to BSU1 phosphatase and GSK3-like kinase BIN2. Mol. Cell *43*, 561–571.

Kim, T.W., Michniewicz, M., Bergmann, D.C., and Wang, Z.Y. (2012). Brassinosteroid regulates stomatal development by GSK3-mediated inhibition of a MAPK pathway. Nature *482*, 419–422.

Ko, R., Park, J.H., Ha, H., Choi, Y., and Lee, S.Y. (2015). Glycogen synthase kinase 3β ubiquitination by TRAF6 regulates TLR3-mediated pro-inflammatory cytokine production. Nat. Commun. *6*, 6765.

Li, J., and Nam, K.H. (2002). Regulation of brassinosteroid signaling by a GSK3/SHAGGY-like kinase. Science *295*, 1299–1301.

Liu, Y.G., Mitsukawa, N., Oosumi, T., and Whittier, R.F. (1995). Efficient isolation and mapping of Arabidopsis thaliana T-DNA insert junctions by thermal asymmetric interlaced PCR. Plant J. *8*, 457–463.

Lu, Q., Tang, X., Tian, G., Wang, F., Liu, K., Nguyen, V., Kohalmi, S.E., Keller, W.A., Tsang, E.W., Harada, J.J., et al. (2010). Arabidopsis homolog of the yeast TREX-2 mRNA export complex: components and anchoring nucleoporin. Plant J. *61*, 259–270.

Oh, E., Zhu, J.Y., Bai, M.Y., Arenhart, R.A., Sun, Y., and Wang, Z.Y. (2014a). Cell elongation is regulated through a central circuit of interacting transcription factors in the Arabidopsis hypocotyl. eLife *3*, e03031.

Oh, E., Zhu, J.Y., Ryu, H., Hwang, I., and Wang, Z.Y. (2014b). TOPLESS mediates brassinosteroid-induced transcriptional repression through interaction with BZR1. Nat. Commun. *5*, 4140.

Peng, P., Yan, Z., Zhu, Y., and Li, J. (2008). Regulation of the Arabidopsis GSK3-like kinase BRASSINOSTEROID-INSENSITIVE 2 through proteasome-mediated protein degradation. Mol. Plant *1*, 338–346.

Peng, P., Zhao, J., Zhu, Y., Asami, T., and Li, J. (2010). A direct docking mechanism for a plant GSK3-like kinase to phosphorylate its substrates. J. Biol. Chem. *285*, 24646–24653.

Schindelin, J., Arganda-Carreras, I., Frise, E., Kaynig, V., Longair, M., Pietzsch, T., Preibisch, S., Rueden, C., Saalfeld, S., Schmid, B., et al. (2012). Fiji: an open-source platform for biological-image analysis. Nat. Methods *9*, 676–682.

Schneider, C.A., Rasband, W.S., and Eliceiri, K.W. (2012). NIH Image to ImageJ: 25 years of image analysis. Nat. Methods *9*, 671–675.

She, J., Han, Z., Kim, T.W., Wang, J., Cheng, W., Chang, J., Shi, S., Wang, J., Yang, M., Wang, Z.Y., and Chai, J. (2011). Structural insight into brassinosteroid perception by BRI1. Nature *474*, 472–476.

Sievers, F., Wilm, A., Dineen, D., Gibson, T.J., Karplus, K., Li, W., Lopez, R., McWilliam, H., Remmert, M., Söding, J., et al. (2011). Fast, scalable generation of high-quality protein multiple sequence alignments using Clustal Omega. Mol. Syst. Biol. *7*, 539.

Sun, Y., Fan, X.-Y., Cao, D.-M., Tang, W., He, K., Zhu, J.-Y., He, J.-X., Bai, M.-Y., Zhu, S., Oh, E., et al. (2010). Integration of brassinosteroid signal transduction with the transcription network for plant growth regulation in Arabidopsis. Dev. Cell *19*, 765–777.

Tang, W., Kim, T.W., Oses-Prieto, J.A., Sun, Y., Deng, Z., Zhu, S., Wang, R., Burlingame, A.L., and Wang, Z.Y. (2008). BSKs mediate signal transduction from the receptor kinase BRI1 in Arabidopsis. Science *321*, 557–560.

Tang, W., Yuan, M., Wang, R., Yang, Y., Wang, C., Oses-Prieto, J.A., Kim, T.-W., Zhou, H.-W., Deng, Z., Gampala, S.S., et al. (2011). PP2A activates brassinosteroid-responsive gene expression and plant growth by dephosphorylating BZR1. Nat. Cell Biol. *13*, 124–131.

Vert, G., and Chory, J. (2006). Downstream nuclear events in brassinosteroid signalling. Nature *441*, 96–100.

Vert, G., Walcher, C.L., Chory, J., and Nemhauser, J.L. (2008). Integration of auxin and brassinosteroid pathways by Auxin Response Factor 2. Proc. Natl. Acad. Sci. USA *105*, 9829–9834.

Wang, Z.Y., Seto, H., Fujioka, S., Yoshida, S., and Chory, J. (2001). BRI1 is a critical component of a plasma-membrane receptor for plant steroids. Nature *410*, 380–383.

Wang, Z.Y., Nakano, T., Gendron, J., He, J., Chen, M., Vafeados, D., Yang, Y., Fujioka, S., Yoshida, S., Asami, T., and Chory, J. (2002). Nuclear-localized BZR1 mediates brassinosteroid-induced growth and feedback suppression of brassinosteroid biosynthesis. Dev. Cell *2*, 505–513.

Wang, Z.Y., Bai, M.Y., Oh, E., and Zhu, J.Y. (2012). Brassinosteroid signaling network and regulation of photomorphogenesis. Annu. Rev. Genet. *46*, 701–724.

Weigel, D., Ahn, J.H., Blázquez, M.A., Borevitz, J.O., Christensen, S.K., Fankhauser, C., Ferrándiz, C., Kardailsky, I., Malancharuvil, E.J., Neff, M.M., et al. (2000). Activation tagging in Arabidopsis. Plant Physiol. *122*, 1003–1013.

Xiong, F., Zhang, R., Meng, Z., Deng, K., Que, Y., Zhuo, F., Feng, L., Guo, S., Datla, R., and Ren, M. (2017). Brassinosteriod insensitive 2 (BIN2) acts as a downstream effector of the target of rapamycin (TOR) signaling pathway to regulate photoautotrophic growth in Arabidopsis. New Phytol. *213*, 233–249.

Yan, Z., Zhao, J., Peng, P., Chihara, R.K., and Li, J. (2009). BIN2 functions redundantly with other arabidopsis gsk3-like kinases to regulate brassinosteroid signaling. Plant Physiol. *150*, 710–721.

Yaron, A., Hatzubai, A., Davis, M., Lavon, I., Amit, S., Manning, A.M., Andersen, J.S., Mann, M., Mercurio, F., and Ben-Neriah, Y. (1998). Identification of the receptor component of the IkappaBalpha-ubiquitin ligase. Nature *396*, 590–594.

Yin, Y., Wang, Z.Y., Mora-Garcia, S., Li, J., Yoshida, S., Asami, T., and Chory, J. (2002). BES1 accumulates in the nucleus in response to brassinosteroids to regulate gene expression and promote stem elongation. Cell *109*, 181–191.

Youn, J.H., and Kim, T.W. (2015). Functional insights of plant GSK3-like kinases: multi-taskers in diverse cellular signal transduction pathways. Mol. Plant *8*, 552–565.

Zhang, Z., Zhu, J.Y., Roh, J., Marchive, C., Kim, S.K., Meyer, C., Sun, Y., Wang, W., and Wang, Z.Y. (2016). TOR signaling promotes accumulation of BZR1 to balance growth with carbon availability in Arabidopsis. Curr. Biol. *26*, 1854–1860.

Zhu, J.Y., Sae-Seaw, J., and Wang, Z.Y. (2013). Brassinosteroid signalling. Development *140*, 1615–1620.

STAR★METHODS

KEY RESOURCES TABLE

REAGENT or RESOURCE	SOURCE	IDENTIFIER
Antibodies		
Mouse monoclonal anti-Myc (9B11)	Cell Signaling Technology	#2276; RRID: AB_2148465
Mouse monoclonal anti-GFP (JL-8)	Clontech	632381; RRID: AB_2313808
Rat monoclonal anti-Tubulin (YL1/2)	Abcam	Ab6; RRID: AB_343284
Rat monoclonal anti-HA	Roche	11867423001; RRID: AB_390919
Mouse monoclonal anti-Ubiquitin (P4D1)	Cell Signaling Technology	3936; RRID: AB_3312929
Rabbit polyclonal anti-BZR1	This paper	Homemade
Rabbit polyclonal anti-BIN2	This paper	Homemade
Chemicals, Peptides, and Recombinant Proteins		
Brassinolide (BL)	Wako	635-00811
Propiconazole (PPZ)	Control Solutions	N/A
Bikinin	ChemBridge	5122035
Lambda protein phosphatase	NEB	P0753
MG132	Sigma-Aldrich	C2211
Critical Commercial Assays		
GFP-nAb Magnetic Agarose Kit	Allele Biotechnology	ABP-NABGFPXK20
Auto-ubiquitinylation kit	Enzo Life Sciences	BML-UW0970-0001
Protein A/G plus agarose	Pierce	20423
TnT quick couple transcription/translation system	Promega	L1170
Spectrum plant total RNA kit	Sigma-Aldrich	STRN250
M-MLV reverse transcriptase	Thermo Fisher Scientific	28025013
Experimental Models: Organisms/Strains		
Arabidopsis: Col-0, Ws	ABRC	
Arabidopsis: *bzr1-1D*	Wang et al., 2002	N/A
Arabidopsis: *bin2-1, bin2-3bil1bil3*	Li and Nam, 2002; Yan et al., 2009	N/A
Arabidopsis: *dwf4*	Choe et al., 1998	N/A
Arabidopsis: *bri1-116*	Wang et al., 2001	N/A
Arabidopsis: *BIN2-ox*	Kim et al., 2009	N/A
Arabidopsis: *KIB1-ox, kib1-cs, kib1-1, KIB1C-ox, KIB1-YFP/bzr1-1D, KIB1-ox/BIN2-ox, KIB1-ox/bin2-1, KIB1::KIB1-YFP, KIB1-GUS*	This paper	N/A
Arabidopsis: *kib1-2*	ABRC	SAIL_1230_F06
Oligonucleotides		
Primers for *KIB1* qRT-PCR F: ATTCGATACTTGCCGTGGAC R: GGATGAGCCATGGAGTTGTT	This paper	Customer order
Primers for *KIB2* qRT-PCR F: TCCAGCTGCTTGAGAGTTGA R: ACAGGCTGCTTTGAATCGTC	This paper	Customer order
Primers for *KIB3* qRT-PCR F: GGTTTTTCCCCACTTTTGGT R: CGTCACTGGTTTTGTCCCTT	This paper	Customer order
Primers for *KIB4* qRT-PCR F: GGAGTCGTTGTTTGGCAAGT R: AACCACAGTCACCGGTTCTC	This paper	Customer order

(*Continued on next page*)

Continued

REAGENT or RESOURCE	SOURCE	IDENTIFIER
Primers for *AT3G03726* qRT-PCR F: CAACGATTTCCACGTTTTGA R: CCACAAAACCGCAGTGTCTA	This paper	Customer order
Primers for *AT4G12800* qRT-PCR F: TCCGACAAGACAACATTCCA R: GGTACGGTATCCAGGGAGGT	This paper	Customer order
Primers for *BIN2* qRT-PCR F: TCTGCTGGTTGTGTTCTTGC R: AAGATCTTGTGCCAGGGATG	This paper	Customer order
Primers for *PP2A* qRT-PCR F: TATCGGATGACGATTCTTCGTGCAG R: GCTTGGTCGACTATCGGAATGAGAG	This paper	Customer order
Primers for *KIB1* promoter cloning F: CACCTCTCCATCTAACACACTAAGCACA R: GGCCAAGTAAAGACCTAGAAACAT	This paper	Customer order
Primers for full length *KIB1* cloning F: CACCATGACACATAAGAAGCAGAAGAAG R: TTAAAGCAACCATTTTGAAGTA	This paper	Customer order
Primer for *KIB1N* cloning R: ACTATGTAGGTTTTGTTTTCATGAGG	This paper	Customer order
Primer for *KIB1C* cloning F:CACCATGAAGAGACCTCGGGTTTGATTTAGTTA	This paper	Customer order
Primers for full length KIB2 cloning F: CACCATGGCGCCTCTCAACTCTCA R: AAGCAACCATTTTCCACCAA	This paper	Customer order
Primers for full length ASK1 cloning F: CACCATGTCTGCGAAGAAGATTGTGTTGAA R: TTCAAAAGCCCATTGGTTCTCTCTGCG	This paper	Customer order
Recombinant DNA		
KIB1::KIB1-YFP	This paper	N/A
35S::KIB1-YFP	This paper	N/A
35S::KIB1-Mys	This paper	N/A
35 s::KIB1C-YFP	This paper	N/A
KIB1-GUS	This paper	N/A
BD-KIB1F, BD-KIB1C, BD-KIB1N, AD-KIB1, AD-KIB2, AD-ASK1	This paper	N/A
AD-BIN2, AD-bin2-1, AD-mBIN2, BD-AtASK11, BD-AtASK12, BD-AtASK13, BD-AtASK22, BD-AtASK23	Kim et al., 2009	N/A
AD-BIN2-GFP	This paper	N/A
AD-KIB1-YFP	This paper	N/A
pXDGATcy86	Ding et al., 2007	N/A
pGADT7-GW	Lu et al., 2010	N/A
pMDC164	Curtis and Grossniklaus, 2003	N/A
Software and Algorithms		
Clustal Omega	Sievers et al., 2011	http://www.clustal.org/omega/; RRID: SCR_001591
ImageJ	Schneider et al., 2012	https://imagej.net/ImageJ; RRID: SCR_003070
Fiji	Schindelin et al., 2012	https://imagej.net/Fiji; RRID: SCR_002285
PHYLIP	Felsenstein, 1989	http://evolution.genetics.washington.edu/phylip/; RRID: SCR_006244

CONTACT FOR REAGENT AND RESOURCE SHARING

Further information and requests for reagents may be directed to and will be fulfilled by the corresponding author, Zhi-Yong Wang (zywang24@stanford.edu).

EXPERIMENTAL MODELS AND SUBJECT DETAILS

All the *Arabidopsis thaliana* plants used in this study were in Col-0 ecotype background, except the *bin2-1 bil2 bil3* mutant which is in Ws ecotype background. The plants were grown in greenhouses with a 16-h light/8-h dark cycle at 22-24°C for general growth and seed harvesting. For seedlings grown on the medium in Petri dishes, the sterilized seeds were grown on 1/2 Murashige and Skoog (MS) medium containing 1% sucrose and supplemented with 0.7% phytoagar. Plates were placed in a growth chamber under the constant light condition at 22°C.

METHOD DETAIL

T-DNA Insertion Mutagenesis and bzr1-1D Suppressor Screen

The *bzr1-1D* mutant plants were transformed with the *pSKI015* plasmid (Weigel et al., 2000) using the floral dipping method (Clough and Bent, 1998). T2 seeds were harvested from each group of 20 T1 plants that showed typical *bzr1-1D* phenotypes (i. e. stem-bending phenotype). About 200 T2 seeds of each pool (average 10 T2 seeds from each T1 line) were grown in the soil at 22-24°C in a green house, and the plants were screened for the lack of the stem-bending phenotype of *bzr1-1D*. The *kib1-1* mutant was isolated after screening T2 seeds from about 2000 T1 lines. The T-DNA flanking sequence was recovered by thermal asymmetric interlaced PCR (TAIL-PCR) (Liu et al., 1995).

Plasmids Construction and Plant Transformation

To generate *KIB1-Myc*, the full-length *KIB1* coding sequence was cloned into the gateway compatible *p1390-4Myc-His* vector. To generate *KIB1-YFP* and *KIB1C-YFP* transgenic lines, the full-length *KIB1* coding sequence or F-box-truncated *KIB1(KIB1C)* sequence with start codon was cloned into the gateway compatible *pX-YFP* vector. To generate *KIB1::KIB1-YFP*, 1.5 kb of KIB1 promoter sequence plus the full-length KIB1 genomic sequence was cloned into the gateway compatible *pEGTW* vector. To generate *KIB1-GUS*, 1.5 kb of KIB1 promoter sequence was cloned into the gateway compatible *pMDC164* vector. Gene specific primers are listed in Key Resource Table.

The resulting vectors were transformed into *Arabidopsis* plants by floral dip (Clough and Bent, 1998). *KIB1-Myc*, *KIB1-YFP*, *KIB1C-YFP* and *KIB1-GUS* constructs were transformed to the wild-type Col-0. *KIB1::KIB1-YFP* construct was transformed to wild-type Col-0 or *kib1-2* mutant.

KIB1-YFP/BIN2-Myc and *KIB1-Myc/BIN2-YFP* transgenic lines were generated by crossing *KIB1-YFP* with *BIN2-Myc* transgenic *Arabidopsis* or crossing *KIB1-Myc* with *BIN2-YFP* transgenic *Arabidopsis*.

Total RNA Extraction and Quantitative RT–PCR Analysis

Total RNA was extracted from seedlings or specific tissues using the Spectrum Plant Total RNA kit. M-MLV reverse transcriptase was used to synthesize cDNA from RNA. Quantitative real-time PCR (qRT-PCR) was performed using LightCycler 480 (Roche) and the Bioline SYBR green master mix. Gene expression levels were normalized to that of *PP2A* and are shown relative to the expression levels in wild-type. Gene specific primers are listed in Key Resource Table.

Co-immunoprecipitation (co-IP) Assays

Plant proteins were extracted using IP buffer (50 mM Tris-Cl pH7.5, 1mM EDTA, 75mM NaCl, 0.1% Triton X-100, 5% Glycerol, 1mM PMSF, 1x Protease Inhibitor). After centrifugation at 20,000 g for 10 min at 4°C, the supernatant was incubated for 1 hr with the GFP-nAb magnetic agarose beads. The beads were then washed for three times with IP buffer. The eluted samples were analyzed by immunoblots using the indicated antibodies.

Yeast Two-Hybrid Assay

The various fragments of *KIB1* cDNA, full-length *KIB2* and *ASK1* were subcloned into the gateway compatible *pGCADT7* or *pXDGATcy86* vector. The constructs were co-transformed into yeast AH109 cells. Yeast clones were grown on the synthetic dropout medium with histidine (+His) or without histidine (-His) containing 3-amino-1, 2, 4-triazole (3-AT, 1mM).

Protein Pull-Down Assays

KIB1-YFP-HA, BIN2-HA, mBIN2-HA, bin2-1-HA or YFP-HA proteins were synthesized by TNT T7 quick coupled in vitro transcription/translation system with the vectors AD-KIB1-YFP, AD-BIN2, AD-bin2-1, and AD-mBIN2. For the pull-down assays using KIB1-YFP-HA as bait, KIB1-YFP-HA proteins were pre-incubated with GFP-nAb magnetic agarose for 1 hr. After removing unbound proteins, BIN2-HA, mBIN2-HA, bin2-1-HA or YFP-HA proteins were incubated with KIB1-YFP-HA immobilized on GFP-nAb magnetic

agarose beads for 1 hr in binding buffer (10 mM Tris-HCl pH 7.5, 150 mM NaCl) at 4°C, and then the beads were washed by the washing buffer (10 mM Tris-HCl pH 7.5, 500 mM NaCl) for three times. The pulled-down proteins were analyzed by immunoblot using an anti-HA antibody.

In Vitro Ubiquitination Analysis

BIN2-GFP-HA and KIB1-HA were synthesized using TnT T7 in vitro transcription/translation system with the vectors AD-BIN2-GFP and AD-KIB1. BIN2-GFP-HA with or without KIB1-HA was incubated in the Ub E3 ligase buffer (50 mM Tris pH 7.6), 0.6 mM DTT, 2 mM Mg-ATP, 1.5 ng/μl E1, 10 ng/μl E2 (UbcH5a), 1 μg/μl ubiquitin, 1 μM histidine-purified recombinant Cullin-1, ASK1 and Rbx1 for 1 hr at 30°C. The ubiquitination products were mixed with the same volume of 2x sample loading buffer were heated at 95°C for 5min and separated by SDS-PAGE and immunoblotted using the anti-HA or anti-Ub antibody. The BIN2-GFP-HA protein was immunoprecipitated from the ubiquitination reaction mixtures using the GFP-nAb magnetic agarose beads. After 1 hr of incubation at 4°C, the beads were washed for three times with wash buffer (10mM Tris-HCl pH 7.5, 500mM NaCl). The immunoprecipitates were eluted using 2X sample loading buffer. Samples were heated at 95°C for 5min and separated by SDS-PAGE and analyzed using anti-HA or anti-Ub antibody.

QUANTIFICATION AND STATISTICAL ANALYSIS

Root and hypocotyl lengths were measured from images using ImageJ software. Band intensity quantification of protein signals from western blot was performed using the ImageJ.

Statistical significance of root and hypocotyl lengths and gene expression were examined by Student's t test (*$p < 0.05$).